Detailed Kinetic Studies of an Aggregating Inhibitor; Inhibition of Phosphomannomutase/Phosphoglucomutase by Disperse Blue 56[†]

Hao-Yang Liu,[‡] Ziaohui Wang,[‡] Catherine Regni,[§] Xiaoqin Zou,*[,‡,§] and Peter A. Tipton*[,§]

Dalton Cardiovascular Research Center and Department of Biochemistry, University of Missouri, Columbia, Missouri 65211

Received April 22, 2004; Revised Manuscript Received May 10, 2004

ABSTRACT: Phosphomannomutase/phosphoglucomutase occupies a central position in the pathways by which several virulence factors are synthesized in *Pseudomonas aeruginosa*. Virtual screening was used to identify potential inhibitors of phosphomannomutase/ phosphoglucomutase, and one compound, the anthraquinone-based dye Disperse Blue 56, showed potent inhibition in vitro. The kinetics of inhibition was complex; the time courses for reactions in the presence of the inhibitor were biphasic, suggestive of slow-binding inhibition. Quantitative analysis of the progress curves and preincubation experiments demonstrated that slow-binding inhibition was not occurring, however. Initial velocity kinetic studies indicated that Disperse Blue 56 was a parabolic, noncompetitve inhibitor. Progress curves for reactions in the presence of Disperse Blue 56 could be fitted very well by a model in which 2 equiv of the inhibitor bound to free enzyme or the enzyme−substrate complex. The inhibition was largely relieved by the inclusion of 0.01% Triton X-100 in the assay solutions, which has been suggested to be the hallmark for inhibition by compounds that exert their effect through aggregates [McGovern, S. L., Caselli, E., Grigorieff, N., and Shiochet, B. K. (2002) *J. Med. Chem. 45*, 1712−1722]. Our kinetic data appear to be consistent with either inhibition by a dimer of Disperse Blue 56 or inhibition by a Disperse Blue 56 aggregate, but the latter appears much more likely. We present a detailed analysis of the system to provide further information that may help in the recognition of inhibition through aggregation.

Recent elegant work by Shoichet and co-workers has called attention to the pervasive problem presented by small organic molecules that appear to be potent enzyme inhibitors but act relatively nonspecifically. The inhibition appears to arise from aggregates of the organic molecules that form in aqueous solution, and Shoichet has called these compounds aggregating inhibitors and discussed some of their inhibitory properties (*2*, *3*). The aggregates that form from the organic molecules are detectable by dynamic light-scattering, and the mechanism by which they inhibit enzymatic reactions appears to involve adsorption of the enzyme onto the surface of the aggregate. Many chemical libraries harbor aggregating inhibitors, so their identification in screening efforts is a significant issue for the pharmaceutical industry.

We have been utilizing virtual screening methods to identify inhibitors of the enzymes involved in alginate biosynthesis in *Pseudomonas aeruginosa*. One of our promising leads was the organic dye Disperse Blue 56, 2-chloro-1,5-diamino-4,8-dihydroxyanthraquinone (Scheme 1), which shows potent inhibition of PMM/PGM,[1] the enzyme that catalyzes the second step in the alginate biosynthetic pathway. Although Disperse Blue 56 was identified by structure-based screening methods, experimental characterization of its action suggests that at least part of its potency may derive from aggregation. We have conducted a kinetic study of Disperse Blue 56 inhibition of PMM/PGM. To our knowledge, this is the first detailed kinetic characterization of an aggregating inhibitor. The results demonstrate that inhibition caused by aggregation can appear quite similar to other modes of inhibitory behavior. Thus, although aggregating inhibitors can be recognized readily when one is predisposed to look for them, the kinetic properties of aggregating inhibitors could also lead one to explain their behavior in terms of more standard kinetic models; we offer the present analysis to help identify some characteristics that may facilitate recognition of aggregating inhibitors.

Scheme 1

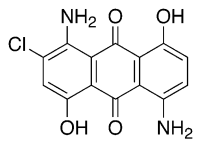

In *P. aeruginosa*, the *algC* gene encodes a phosphohexose mutase designated PMM/PGM that exhibits equal specificity for mannose 6-P and glucose 6-P (*4*, *5*). The phosphomannomutase activity of PMM/PGM generates mannose 1-P, which is required for alginate biosynthesis; alginate is an

[†] This work was supported by a grant to P.A.T. from the National Institutes of Health (GM59653) and AHA Grant 0265293Z (Heartland Affiliate), NIH Grant DK61529, and a grant from the Research Board of the University of Missouri to X.Z.

* To whom correspondence should be addressed. (P.A.T.) Telephone: (573) 882-7968. Fax: (573) 442-4812. E-mail: tiptonp@missouri.edu. (X.Z.) Telephone: (573) 882-6045. Fax: (573) 884-4232. E-mail: zoux@missouri.edu.

[‡] The Dalton Cardiovascular Research Center.

[§] The Department of Biochemistry.

[1] Abbreviations: PMM/PGM, phosphomannomutase/phosphoglucomutase; DB, Disperse Blue 56; ACD, Available Chemicals Directory; MOPS, 3-(*N*-morpholino)-propane sulfonic acid; DTT, dithiothreitol.

10.1021/bi0491907 CCC: $27.50
Published on Web 06/16/2004

exopolysaccharide secreted by the bacteria, which serves a protective function against antibiotics and the host immune response. The phosphoglucomutase activity forms glucose 1-P, which is an intermediate in lipopolysaccharide and rhamnolipid biosynthesis. *P. aeruginosa* is an opportunistic pathogen that does not respond well to conventional antibiotic treatment; it poses a particular threat to cystic fibrosis patients and patients with compromised immune systems (*6*). Alginate, lipopolysaccharide, and rhamnolipids are all virulence factors that play roles in *Pseudomonas* infections. Because PMM/PGM is required for the biosynthesis of all three compounds, it is a uniquely attractive target for drug development.

Extensive crystallographic studies have revealed the interactions between active-site residues and the substrates and products that enforce the specificity of the PMM/PGM reaction while still allowing two different substrates and two different products to bind at the same active site (*7*). Importantly, the structural data also provide the starting point for computer-aided searches for potential inhibitors. Kuntz and co-workers have developed the program DOCK as a means to explore potential binding interactions between proteins and ligands (*8*). Combining DOCK with a virtual library of chemical compounds and a specified scoring function allows one to identify potential inhibitors for any enzyme whose structure is known. Screening the Available Chemicals Directory database against the structure of PMM/PGM led to the prediction that Disperse Blue 56 should be a good ligand. In fact, Disperse Blue 56 showed potent inhibiton of PMM/PGM, but the kinetic behavior was relatively complex.

MATERIALS AND METHODS

Computational Methods. The DOCK software (*8*) and an implemented pairwise GB/SA scoring function (*9*) were used to screen the ACD database (MDL, Inc.) for potential inhibitors. First, the active site of PMM/PGM was chosen as the potential binding site and was characterized. The crystal structures of PMM/PGM in complex with the substrates glucose 6-P and mannose 6-P and the products glucose 1-P and mannose 1-P are all very similar (*7*) (PDB code 1P5D; (*10*)). A complex with the inhibitor xylose 1-P bound was used in our modeling calculations. The water molecules and the xylose 1-P molecule were removed from the crystal structure. The Zn atom was replaced by a catalytic Mg atom and was treated as part of the protein. The Amber protein parameters (*11*) were used for charge and atom type assignments for the protein via the Sybyl software (Tripos, Inc). On the basis of the phosphorylation state of the catalytic serine, S108, two forms of PMM/PGM were considered: the phosphorylated form and the dephosphorylated form. The SPHGEN program in the DOCK software was used to generate the negative image of the active site of PMM/PGM for the docking process.

Second, each compound from the ACD database (MDL Information Systems, Inc.) was docked into the active site of PMM/PGM and scored with the pairwise GB/SA scoring function. The initial conformation of each compound was generated using the CONCORD algorithm (*12*). Both rigid docking and flexible docking were performed. The top 200 ligands were examined visually using the MidasPlus program (*13*). Selected compounds were purchased and tested as inhibitors of PMM/PGM.

Scheme 2

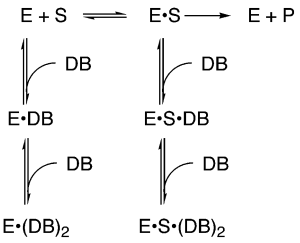

Materials. PMM/PGM was obtained from *Escherichia coli* cells that overexpress the *algC* gene, as previously described (*14*). The PMM/PGM that was used in these studies has a $(His)_6$-tag at the N-terminus to facilitate purification. The tag has no influence on the kinetic characteristics of the enzyme. Glucose 1-P, glucose 1,6-P_2, NAD^+, and *Leuconostoc mesenteroides* glucose 6-P dehydrogenase were obtained from Sigma. Glucose 1-P was purified by anion exchange chromatography to remove contaminating glucose 1,6-P_2 (*15*). Disperse Blue 56 was obtained from Aldrich and was used without further purification. Mass spectral and ^1H NMR analysis revealed that the commercial preparation was a 7:3 mixture of nonhalogenated to halogenated material.

Kinetic Assays. The PMM/PGM reaction was followed in the reverse of the biosynthetic direction using a coupled assay with glucose 6-P dehydrogenase. All spectrophotometric assays were conducted at 25 °C in 1 mL cuvettes using a Varian 50 Bio spectrophotometer. Unless otherwise noted, reactions were initiated by the addition of PMM/PGM to the cuvette. Reactions were conducted in 50 mM MOPS, pH 7.4, containing 1 mM DTT, 1.5 mM $MgSO_4$, 0.9 mM NAD^+, and variable amounts of glucose 1-P. The activator glucose 1,6-P_2 was not present in these assays, unless explicitly noted.

Experiments in which PMM/PGM was preincubated with the inhibitor were conducted in a volume of 50 μL; 3.3 μM PMM/PGM was incubated with 10 μM Disperse Blue 56 in the presence and absence of 2 mM $MgSO_4$ and 5.3 μM glucose 1-P. After a 1 h incubation at room temperature, a 10 μL aliquot was removed from each reaction mixture and diluted into a 1 mL cuvette containing the components of the standard coupled assay. The 100-fold dilution reduced the concentration of Disperse Blue 56 below inhibitory levels.

Dynamic Light Scattering. Solutions of Disperse Blue 56 were characterized by dynamic light scattering using a Protein Solutions DynaPro 99 instrument. The Disperse Blue was prepared as a stock solution in DMSO and diluted into filtered 100 mM MOPS, pH 7.4 for the measurements. Immediately prior to data collection, samples were vortexed for 5 s to ensure an even distribution of particles. At least 20 measurements were taken on each sample.

Data Analysis. The time courses for the PMM/PGM reaction in the presence of Disperse Blue 56 were fitted to eq 1, where P is the product, v_o is the initial velocity of the reaction, v_s is the steady-state velocity that it reaches, and k is the rate constant for the transition between the two kinetic phases. Values for k that were obtained from eq 1 were evaluated using eq 2, which describes the relationship between k and the rate constants for interconversion of the inhibitory complexes that are shown in Scheme 2 (*16*). Initial

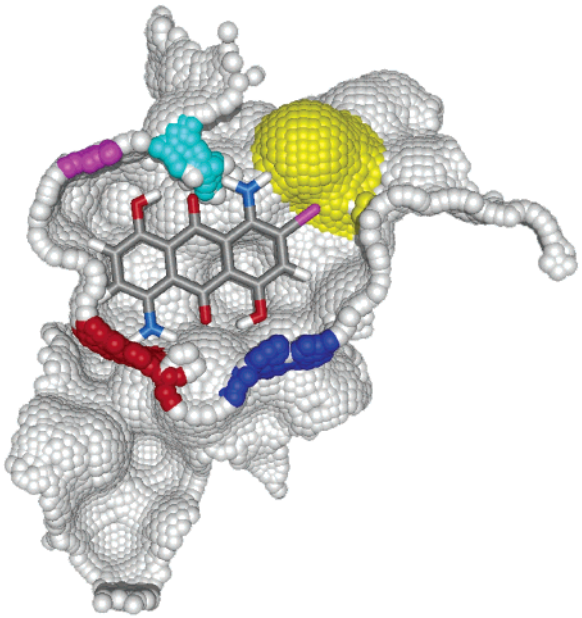

FIGURE 1: Predicted binding mode for DB in the active site of dephospho-PMM/ PGM. The DB molecule is displayed in stick mode and colored by atom type (red for O, blue for N, gray for C, white for H, and magenta for halogen). The molecular surface of PMM/PGM is colored in gray except the residues that may potentially form hydrogen bonds with DB: S108, magenta; H109, cyan; K285, blue; E325, red; and T426, yellow. The figure was prepared with the MidasPlus software (UCSF).

velocity kinetics data were fitted to eq 3, which describes parabolic, noncompetitive inhibition. In eq 3, K_{is1} and K_{ii1} are the dissociation constants for the inhibitor from the E·I and E·S·I complexes, respectively, and K_{is2} and K_{ii2} are the dissociation constants for the second equivalent of inhibitor from the E·$(I)_2$ and E·S·$(I)_2$ complexes, respectively.

$$P = v_s t + (v_o - v_s)(1 - e^{-kt})/k \quad (1)$$

$$k = k_6 + k_5\left(\frac{I/K_i}{1 + A/K_m + I/K_i}\right) \quad (2)$$

$$Y = \frac{VA}{K\left(1 + \frac{I}{K_{is1}} + \frac{I^2}{K_{is2}}\right) + A\left(1 + \frac{I}{K_{ii1}} + \frac{I^2}{I_{ii2}}\right)} \quad (3)$$

Numerical fitting of progress curves to various models for the enzymatic reaction was performed using the program Dynafit (*17*).

RESULTS

Virtual screening of the ACD database suggested several dozen compounds that might be inhibitors of PMM/PGM. Forty compounds were obtained and tested experimentally; Disperse Blue 56 was identified as a potential ligand to dephospho-PMM/PGM (Figure 1). In assays of PMM/PGM activity it showed potent inhibition and was therefore characterized further. No inhibition was observed when the analogue of DB lacking a halogen, 1,5-diamino-4,8-dihydroxyanthraquinone, was tested. Time courses for reaction in the presence of Disperse Blue 56 are illustrated in Figure 2; it is apparent that inhibition is a time-dependent phenomenon. To determine if the time-dependent inhibition arose

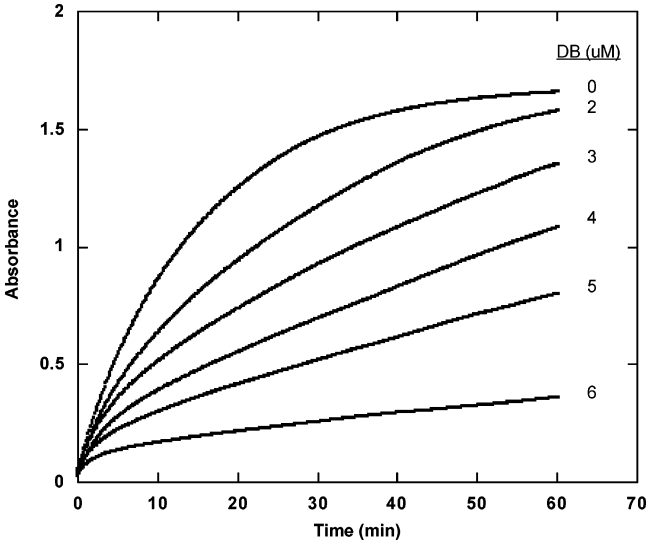

FIGURE 2: Timecourses for product formation in the presence of Disperse Blue 56. Assay conditions are given in the text; each reaction was initiated by the addition of 3.3 μg PMM/PGM.

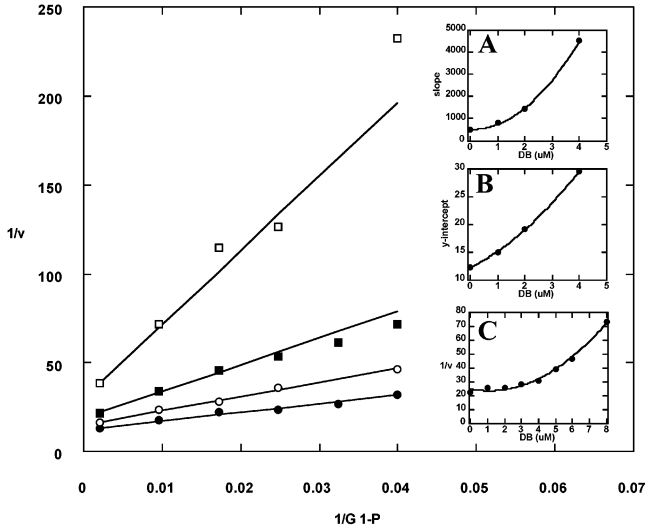

FIGURE 3: Initial velocity kinetics data for the PMM/PGM reaction in the absence of Disperse Blue 56 (●) and at 1 μM (○), 2 μM (■), and 4 μM (□). The points are experimental, and the lines are the fit to eq 3. Insets: (A) slope replots from individual data sets collected at each Disperse Blue 56 concentration and fitted to the Michaelis−Menten equation. (B) Intercept replots from individual data sets collected at each Disperse Blue 56 concentration and fitted to the Michaelis−Menten equation. (C) Initial velocities in the presence of 500 μM glucose 1-P, and Disperse Blue, as shown.

from slow binding and slow release of the inhibitor, PMM/PGM was preincubated with Disperse Blue 56 and then assayed after diluting out the inhibitor. Regardless of whether the enzyme was incubated with Disperse Blue 56 alone or in the presence of Mg^{2+} and glucose 1-P no lag in product formation was observed upon addition of the enzyme−inhibitor complex to the assay solution (data not shown).

In addition to the slow onset inhibition, Disperse Blue 56 also affected the initial velocity of PMM/PGM-catalyzed reactions. The initial velocity data are shown in Figure 3 in the form of a reciprocal plot. Replots of the slopes and intercepts for the data obtained at each inhibitor concentration were nonlinear (Figure 3A,B). To confirm the nonlinear nature of the inhibition, initial velocities were measured at 500 μM glucose 1-P at a number of different inhibitor

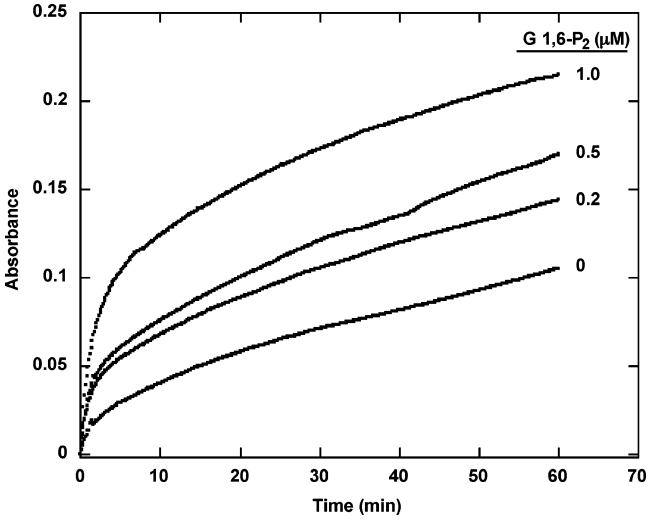

FIGURE 4: Effect of glucose 1,6-P_2 on the PMM/PGM reaction in the presence of Disperse Blue 56. Reaction conditions are given in the text; each reaction was initiated by the addition of 3.3 μg of PMM/PGM.

concentrations. As shown in Figure 3C, the reciprocals of the initial velocities were clearly nonlinear with respect to Disperse Blue 56 concentration, confirming the parabolic nature of the inhibition (*18*). The entire family of data in Figure 3 was fitted to eq 3, which describes parabolic, noncompetitive inhibition. The values obtained from this analysis were K_{is1} 5.0 ± 3.6, K_{is2} 2.4 ± 0.4, K_{ii1} 5.6 ± 1.4, and K_{ii2} 20 ± 7 μM.

The effect of glucose 1,6-P_2 on DB inhibition was investigated. As shown in Figure 4, glucose 1,6-P_2 increases the amplitude of the burst phase that occurs prior to onset of the slow, inhibited phase of the reaction. Although it is not readily apparent from the figure because the substrate became depleted at high glucose 1,6-P_2 concentrations before the steady-state velocity was achieved, fitting the time course to eq 1 suggested that glucose 1,6-P_2 also relieved the inhibition of the steady-state phase of the reactions as well.

Shoichet and co-workers have suggested that relief of inhibition by Triton X-100 can be used as a criterion to identify aggregating inhibitors (*3*). In fact, the presence of 0.01% Triton X-100 did reduce the inhibitory behavior of DB quite significantly. At 6 μM DB, the steady-state velocity of the PMM/PGM reaction was reduced to 15% of that in the absence of inhibitor, but when 0.01% Triton X-100 was present, the steady-state velocity was 75% that of the control reaction in which DB was absent. Thus, although DB does still show inhibition toward PMM/PGM in the presence of Triton X-100, it appears that DB derives much of its potency from acting in an aggregated or multimeric form.

Another unique feature of aggregating inhibitors is that inhibition is attenuated as the enzyme concentration increases (*2*). Under the standard conditions used in the experiments reported here, PMM/PGM was present at 3.3 μg/mL, and when assayed in the presence of 265 μM glucose 1-P, the apparent IC_{50} for DB was approximately 5 μM. When the PMM/PGM concentration was increased to 33 μg/ mL, no inhibition by DB was observed, up to a concentration of 10 μM.

Dynamic light scattering measurements demonstrated that DB exists as an aggregate in aqueous solution. At a nominal concentraton of 10 μM, the DB solution contained a broad range of particles whose mean radius was 43.4 nm and mean molecular mass was 32 000 kDa; the polydispersity index was 0.51, and the average intensity of the light scattering was 92.4 kilocounts per second. A 50 μM solution of DB contained particles whose mean radius was 134.2 nm and mean molecular mass was 2 000 000 kDa. The solution was quite heterogeneous, indicated by a polydispersity index of 0.67, and the average intensity of the light scattering was 808.3 kilocounts per second.

DISCUSSION

P. aeruginosa is an opportunistic pathogen that poses severe risks for many patient groups, including those who must endure prolonged hospital stays, immunocompromised patients, and cystic fibrosis patients (*19*). Several factors contribute to the pathogenicity of *P. aeruginosa*, including the production of alginate and the biofilm mode of growth that mature bacterial populations adopt. *P. aeruginosa* growing in the biofilm mode exhibit greatly reduced sensitivity to antibiotic treatment, compared to those growing in the planktonic state. This suggests that compounds that interfere with biofilm formation, and the production of constituents of the biofilm may be useful in the treatment of *P. aeruginosa* infections. PMM/PGM plays a central role in the biosynthesis of three distinct virulence factors: alginate, rhamnolipid, and lipopolysaccharide. For this reason, it is an attractive target for drug design.

Rational drug design may proceed by defining the transition state for the catalytic process and then preparing stable compounds that act as transition state mimics (*20*). In the case of PMM/PGM, it is difficult to mimic the transition state for phosphoryl transfer with stable compounds.[2] An alternative to transition state analogue design is to utilize available structural information to identify ligands that are predicted to bind in the enzyme active site. A number of computational methods have been developed for evaluating protein−ligand interactions, and this methodology has the advantage of being easily adapted to virtual screening of various chemical compound databases.

By screening the ACD database against the structure of dephospo-PMM/PGM, Disperse Blue 56 was identified as a potential ligand. The predicted binding mode of DB is somewhat different from the binding mode of the natural substrate glucose 1-P that is observed in the crystal structure of the phospho-PMM/PGM-glucose 1-P complex (*7*). DB is predicted to form hydrogen bonds with S108, K285, and E325, as does glucose 1-P. Further, DB may potentially form hydrogen bonds with H109 and T426 (Figure 1). Glucose 1-P forms hydrogen bonds with H308, R421, and N424, but these residues are predicted not to interact with DB.

The predicted inhibition of PMM/PGM by DB was borne out experimentally. However, the kinetic behavior of PMM/PGM in the presence of DB turned out to be more complex than might have been expected. The relief of the inhibition in the presence of Triton X-100, and the sensitivity of the

[2] Vanadate esters, which form spontaneously and nonspecifically between vanadate and hydroxyl groups on carbohydrates, have often been found to inhibit enzymes catalyzing phosphoryl transfer. Although vanadate is a potent inhibitor of rabbit muscle PGM (*1*), it has little effect on PMM/PGM (P. Tipton, unpublished observations).

Scheme 3

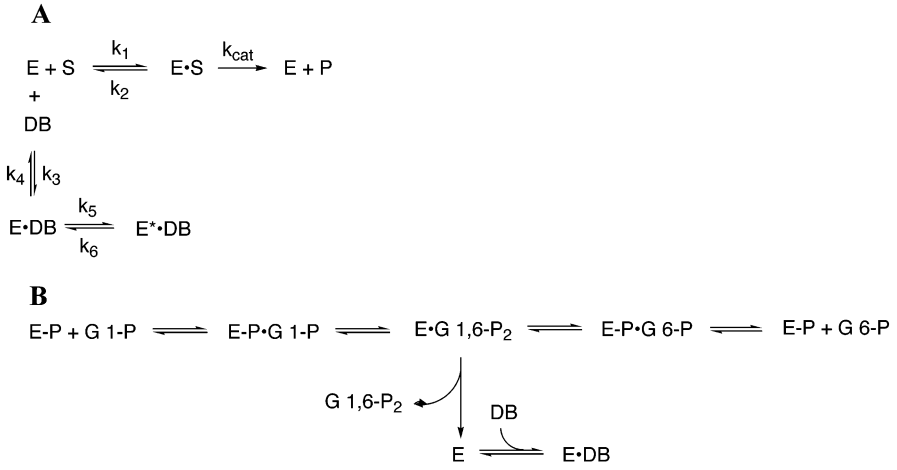

inhibition to protein concentration strongly suggest that the potency of the inhibition derives from properties of multimeric forms of DB, or a DB aggregate. However, this possibility was not immediately apparent to us, and our analysis of the kinetics of DB inhibition show that inhibition by aggregation of the inhibitor may be interpreted in terms of other models that are more familiar to enzymologists.

Consideration of the structure of DB clearly suggests a mechanism by which it can aggregate; the functional groups can hydrogen bond to form an infinite two-dimensional array, or π-stacking may lead to aggregation. Nonetheless, some properties of the system did not make it an obvious candidate as an aggregating inhibitor. DB is quite soluble in water, at least initially, although precipitates can be observed to form over time. Although aggregating inhibitors are usually nonspecific, DB appeared not inhibit the coupling enzyme used in the assay, glucose 6-phosphate dehydrogenase. 3-[(4-Phenoxyanilino)methylene]-2-benzofuran-1(3*h*)-one, which has been characterized as a nonspecific aggregating inhibitor when assayed with β-lactamase (*3*), did not show significant inhibition of PMM/PGM (data not shown). Finally, glucose 1,6-P_2 relieved the inhibition by DB; we do not yet understand the mechanism underlying the effect of glucose 1,6-P_2. These results suggest, perhaps not surprisingly, that although aggregating inhibitors do act relatively nonspecifically, individual enzymes will vary in their sensitivity to inhibition.

Because more and more aggregating inhibitors are likely to be identified, we believe that it is useful to present a detailed kinetic analysis of a system in which aggregation behavior is a contributing factor to the observed inhibition. This should not only provide insights into the mechanisms of action of such inhibitors but also provide guidelines to facilitate their recognition.

The inhibition of PMM/PGM by DB was clearly a time-dependent process, that is, the potency of the inhibition appeared to increase during the course of the reaction. The result, as illustrated in Figure 2, was biphasic time courses, in which the steady-state velocity was not achieved until after 10−20 min of reaction. Close examination of the early portions of the time course revealed that the initial velocities of the reactions were also inhibited by DB. Therefore, our analysis of DB inhibition began by defining the mode of inhibition observed in the initial velocities.

The reciprocal plots obtained with glucose 1-P as the variable substrate in the absence of glucose 1,6-P_2 and in the presence of DB defined a family of intersecting lines with distinct *y*-intercepts. The inhibition pattern indicated that DB acts as a noncompetitive inhibitor versus glucose 1-P. If DB bound only to the same enzyme form as glucose 1-P (i.e., phosphorylated PMM/PGM), it would be predicted to act as a competitive inhibitor. Conversely, if it acted as a dead-end inhibitor that bound only to the enzyme−substrate complex or enzyme−intermediate complex, it should act as an uncompetitive inhibitor. The observed noncompetitive inhibition suggests that DB can bind to both the free enzyme, affecting the slopes of the reciprocal plots, and to the enzyme−substrate or enzyme−intermediate complex, affecting the intercepts of the reciprocal plots. Thus, the predicted binding mode of DB shown in Figure 1 is not consistent with its apparent binding to the phosphorylated form of the enzyme, nor is it consistent with conclusion that at least 2 equiv of DB (vide infra) are required for potent inhibition.

The slope and intercept replots of the DB inhibition data were nonlinear (Figure 3A,B). The points fitted well to a parabolic function, suggesting that 2 equiv of inhibitor bind to the enzyme (*18*). The parabolic inhibition was confirmed by measuring the velocity of the reaction under saturating conditions as a function of DB concentration (Figure 3C). The steady-state kinetic mechanism suggested by these data is shown in Scheme 2. It is worth considering whether parabolic inhibition can arise from aggregation of the inhibitor. Eq 3 accounts for parabolic inhibition through the squared terms for inhibitor concentration in the denominator of the function. The function describing inhibition by an aggregate of the inhibitor should contain higher order terms, up to the number of inhibitor molecules in the aggregate. As can be seen from Figure 3, the simpler model fits the data quite well. However, if additional, higher order terms were to be added to eq 3, the data would have to be fitted at least as well (since adding additional parameters to the function would not decrease the quality of the fit). Probably the most reasonable way to view the data is to recognize that K_{i1} and K_{i2} are apparent inhibition constants that contain contributions from a variety of inhibitory species.

We initially considered two mechanisms to explain the shape of the PMM/PGM timecourses in the presence of DB

(Scheme 3). The classic explanation for time-dependent inhibition, such as that shown in Figure 2, is that it results from slow isomerization of the initial enzyme−inhibitor complex, to a second, more stable complex, from which the inhibitor dissociates only very slowly (*16*) (Scheme 3A). An alternative explanation for the observed inhibition of PMM/PGM is that DB inhibition arises from preferential binding to the dephospho form of the enzyme that is generated during turnover. During the catalytic cycle, PMM/PGM donates a phosphoryl group to the substrate to generate a bisphosphorylated intermediate. Infrequently, the intermediate dissociates from the enzyme active site, leaving dephosphorylated enzyme that is catalytically incompetent until it is rephosphoryated by glucose 1-P, glucose 6-P, or glucose 1,6-P_2.[3] If DB were to trap the dephosphorylated enzyme and prevent its rephosphorylation, it would have the effect of inhibiting the reaction (Scheme 3B). Since DB was identified through virtual screens against the dephosphorylated form of PMM/PGM, we initially considered that the previous scenario was a likely cause of the observed inhibition.

Slow-binding inhibition does not seem to be occurring with DB, based on several observations. First, we analyzed the progress curves in the presence of DB using eq 1 to obtain values for k, the rate constant for the interconversion between the initial velocity and the steady-state velocity of the reaction. Eq 2 describes the relationship between k and the rate constants for interconversion of the two enzyme−inhibitor complexes, k_5 and k_6. It can be seen that k should be a linear function of the quantity that multiplies k_5 in eq 2. However, a plot of k versus $(I/K_i)/(1 + A/K_m + I/K_i)$ was nonlinear, and linear extrapolation to the y-axis, which should represent k_6, provided a negative value.

More direct evidence against the model in Scheme 3A was provided by a preincubation experiment in which PMM/PGM was incubated with DB for 1 h and then diluted into a solution containing substrate. If the observed potent inhibition were due to slow release of DB from the EI* complex, a slow return of activity, which provides a direct measure of k_6, should have been observed. In fact, no lag in activity was apparent; enzyme incubated with DB in the absence of substrate, or in the presence of Mg^{2+} alone or in combination with glucose 1-P, showed identical activity with a control sample that had been incubated in the absence of DB. Thus, slow-binding inhibition did not seem to be the basis for the inhibition of PMM/PGM by DB.

To evaluate whether trapping of dephosphorylated enzyme, as shown in Scheme 3B, provides a more satisfactory explanation of the experimental data, we examined the effect of added glucose 1,6-P_2 on DB inhibition. If DB traps the dephosphorylated enzyme, one would predict that glucose 1,6-P_2 would relieve DB inhibition. In fact, it can be seen in Figure 4 that glucose 1,6-P_2 greatly stimulates the burst phase of the reaction. It is more difficult to gauge the effect of glucose 1,6-P_2 on the steady-state velocity of the reactions because at the higher concentrations of glucose 1,6-P_2 the substrate became depleted before the steady-state phase of the reaction was reached. (It was not possible to use higher concentrations of glucose 1-P in these experiments because of substrate inhibition arising from competition between glucose 1-P and glucose 1,6-P_2 for dephospho-enzyme.) However, fitting the timecourses to eq 1 yielded values for v_s that increased with increasing glucose 1,6-P_2. These observations are qualitatively consistent with the mechanism for inhibition that is shown in Scheme 3B.

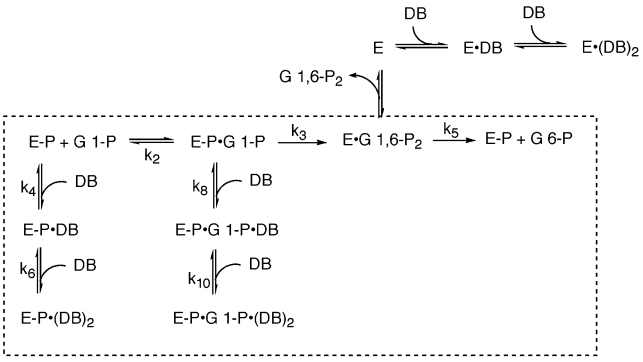

FIGURE 5: Kinetic model used to fit progress curves for the PMM/PGM reaction in the presence of Disperse Blue 56. The section of the model enclosed in the box was sufficient to yield a good fit.

Because of the complicated nature of the relationship between activation of PMM/PGM by glucose 1,6-P_2 and substrate inhibition by glucose 1-P, as well as the apparent time-dependent and parabolic nature of the inhibition by DB, we sought to evaluate the mechanistic possibilities for inhibition by fitting the experimental time courses to different models utilizing the computer program Dynafit (*17*). A model incorporating DB binding to free enzyme, enzyme−substrate, and enzyme−inhibitor complexes was constructed (Figure 5). The model also incorporated the sequential binding of two molecules of inhibitor to each complex. The experimental data were fitted to the model quite satisfactorily; we then proceeded to eliminate portions of the model and evaluate whether the remaining portions were sufficient to obtain a good fit. (We have focused on reproducing the DB concentration dependence and the shape of the time courses; we do not consider the values of the rate constants that were obtained through the analysis to be significant since the data were collected at a single substrate concentration and the number of rate constants in the model is far too high to allow them to be determined uniquely.) We found that eliminating from the model the steps that described the binding of the second equivalent of DB precluded obtaining satisfactory fits. However, removing the branch of the mechanism that described binding of DB to the dephosphoenzyme−intermediate complex had no effect on convergence to a qualitatively satisfactory fit (Figure 6). Thus, all of the properties of DB inhibition can be explained by a model in which 2 equiv of DB serve as the true inhibitory species.

Shoichet has pointed out that aggregating inhibitors can be recognized readily by adding an agent to disperse the aggregate; Triton X-100 appears to be particularly useful. Triton X-100 relieves most of the inhibition of PMM/PGM by DB; on the basis of these data, and the observation that DB forms aggregates that are detectable by light-scattering, we concluded that DB derives at least some of its potency by acting as an aggregating inhibitor. This conclusion was substantiated by the observation that DB inhibition disappears at higher concentrations of PMM/PGM. These considerations suggest that although our kinetic data can be explained by parabolic, noncompetitive inhibition involving 2 equiv of DB,

[3] Kinetic studies indicate that glucose 1,6-P_2 dissociates from PMM/PGM once every 14 cycles (P. Tipton, manuscript in preparation).

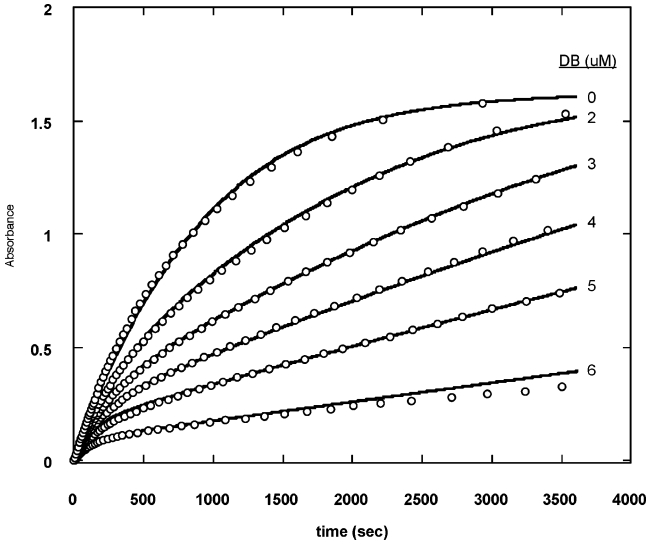

FIGURE 6: Results of fitting experimental timecourses to the kinetic model shown in Figure 4. The data points (○) are the same as those shown in Figure 1, but only 10% of the points are shown to facilitate a comparison between experimental and fitted timecourses. The fitted timecourses are shown as solid lines. All bimolecular rate constants were set at 1 μM^{-1} s^{-1}; k_3 and k_5 were fixed at 25.2 and 3000 s^{-1}, respectively. Values for k_6 and k_8 were poorly determined by the fit, so they were fixed at 800 and 0.13 s^{-1}, respectively, in the final fitting. The values determined by the fit were k_2 1249 ± 4, k_8 398 ± 63, and k_{10} $9.6 \times 10^{-4} \pm 7 \times 10^{-6}$ s^{-1}.

it is much more likely that inhibition arises from aggregates of DB.

It is worthwhile to reiterate the kinetic properties that DB inhibition exhibited; it would be interesting to examine other aggregating inhibitors to determine whether these are general. First, the time courses were biphasic, suggestive of slow binding inhibition. However, quantitative analysis of the progress curves showed that the dependence of the observed rate constant k in eq 2 on inhibitor concentration was not linear. Extrapolations of the data to zero inhibitor concentration yielded a negative value for the rate constant for conversion of the putative EI* complex back to EI. Preincubation experiments directly demonstrated that slow binding inhibition was not occurring because there was no lag in the achievement of the steady-state velocity upon dilution of the inhibitor. The initial velocity kinetic data were fitted well by the function describing parabolic, noncompetitive inhibition. The nonlinear nature of the relationship between reaction velocity and inhibitor concentration is another clue that inhibition via aggregation may be occurring. This brings up a possible ambiguity that emerges from the kinetics experiments; in the absence of other data, it is difficult to distinguish between aggregating inhibition and inhibition that arises from a dimer of the inhibitor. If the inhibitory species is truly a DB dimer, then its potency must be exquisite since it is likely to be a minor component of the DB solution. On the other hand, the apparent potent inhibition suggested by the Dynafit analysis (K_d for the dissociation of DB from the E−P•G 1−P•$(DB)_2$ complex, ∼1 nM) is more likely to be the product of many dissociation constants representing many different inhibitory species. This inhibition constant cannot be compared directly to those derived from eq 3 since they report on the initial velocity portion of the reaction only. In general, it would seem that when parabolic inhibition, or time-dependent inhibition that is not linearly dependent on inhibitor concentration, is observed, it would be prudent to consider whether the system under investigation may be prone to aggregation behavior. Addition of a detergent to disperse the aggregate and determination of the sensitivity of inhibition to enzyme concentration are simple experiments that should be performed to help clarify the origin of the inhibition.

ACKNOWLEDGMENT

We are grateful to Dr. Agoston Jerga for chemical analysis of Disperse Blue 56 samples. Support from Tripos, Inc. (St. Louis, MO) and MDL Information Systems, Inc. (San Leandro, CA) to X.Z. is gratefully acknowledged.

REFERENCES

1. Percival, M. D., Doherty, K., and Gresser, M. J. (1990) Inhibition of phosphoglucomutase by vanadate, *Biochemistry 29*, 2764−2769.
2. McGovern, S. L., Caselli, E., Grigorieff, N., and Shoichet, B. K. (2002) A common mechanism underlying promiscuous inhibitors from virtual and high-throughput screening, *J. Med. Chem. 45*, 1712−1722.
3. McGovern, S. L., Helfand, B. T., Feng, B., and Shoichet, B. K. (2003) A specific mechanism of nonspecific inhibition, *J. Med. Chem. 46*, 4265−4272.
4. Ye, R. W., Zielinski, N. A., and Chakrabarty, A. M. (1994) Purification and characterization of phosphomannomutase/phosphoglucomutase from *Pseudomonas aeruginosa* involved in biosynthesis of both alginate and lipopolysaccharide, *J. Bacteriol. 176*, 4851−4857.
5. Naught, N. E., and Tipton, P. A. (2001) Kinetic mechanism and pH dependence of the kinetic parameters of *Pseudomonas aeruginosa* phosphomannomutase/phosphoglucomutase, *Arch. Biochem. Biophys. 396*, 111−118.
6. Yu, H., and Head, N. E. (2002) Persistent infections and immunity in cystic fibrosis, *Frontiers Biosci. 7*, 442−457.
7. Regni, C., Naught, L., Tipton, P. A., and Beamer, L. J. (2004) Structural basis of diverse substrate recognition by the enzyme PMM/PGM from *Pseudomonas aeruginosa*, *Structure 12*, 1−20.
8. Ewing, T. J. A., and Kuntz, I. D. (1997) Critical evaluation of search algorithms for automated molecular docking and database screening, *J. Comput. Chem. 18*, 1175−1189.
9. Liu, H.-Y., Kuntz, I. D., and Zou, X. (2004) Pairwise GB/SA scoring function for structure-based drug design, *J. Phys. Chem. B 108*, 5453−5462.
10. Berman, H. M., Westbrook, J., Feng, Z., Gilliland, G., Bhat, T. N., Weissig, H., Shindyalov, I. N., and Bourne, P. E. (2000) The protein data bank, *Nucleic Acids Res. 28*, 235−242.
11. Weiner, S. J., Kollman, P. A., Case, D. A., Singh, U. C., Ghio, C., Alagona, G., Prefeta, S., Jr., and Weiner, P. (1984) A new force field for molecular mechanical simulation of nucleic acids and proteins, *J. Am. Chem. Soc. 106*, 765−784.
12. Rusinko, A., III, Sheridan, R. P., Nilakantan, R., Nilakantan, K. S., Bauman, N., and Venkataraghavan, R. (1989) Using CONCORD to construct a large database of three-dimensional coordinates from connection tables, *J. Chem. Inf. Comput. Sci. 29*, 251−255.
13. Ferrin, T. E., Huang, C. C., Jarvis, L. E., and Langridge, R. (1988) The MIDAS display graphic system, *J. Mol. Graphic 6*, 13−27.
14. Naught, L. E., Regni, C., Beamer, L. J., and Tipton, P. A. (2003) Roles of active site residues in *Pseudomonas aeruginosa* phosphomannomutase/ phosphoglucomutase, *Biochemistry 42*, 9946−9951.
15. Ray, W. J. J., Burgner, J. W. N., and Post, C. B. (1990) Characterization of vanadate-based transition-state analogue complexes of phosphoglucomutase by spectra and NMR methods, *Biochemistry 29*, 2770−2778.
16. Morrison, J. F., and Walsh, C. T. (1987) The behavior and significance of slow-binding enzyme inhibitors, *Adv. Enzymol. Relat. Areas. Mol. Biol. 61*, 201−301.
17. Kuzmic, P. (1996) Program DYNAFIT for the analysis of enzyme kinetic data: application to HIV proteinase, *Anal. Biochem. 237*, 260−273.

18. Cleland, W. W. (1970) Steady-state kinetics, in *The Enzymes* (Boyer, P. D., Ed.) pp 1−65, Academic Press, New York.
19. Wilson, R., and Dowling, R. B. (1998) Lung infections 3. *Pseudomonas aeruginosa* and other related species, *Thorax 53*, 213−219.
20. Schramm, V. L., Horenstein, B. A., and Kline, P. C. (1994) Transition State Analysis and Inhibitor Design for Enzymatic Reactions, *J. Biol. Chem. 269*, 18259−18262.

BI0491907